IOP Publishing Journal of Physics: Condensed Matter

J. Phys.: Condens. Matter **22** (2010) 414102 (9pp) doi:10.1088/0953-8984/22/41/414102

Polyelectrolyte-mediated bridging interactions: columnar macromolecular phases

Matjaž Ličer[1] **and Rudolf Podgornik**[2,3]

[1] Department of Physics, Faculty of Mathematics and Physics, University of Ljubljana, SI-1000 Ljubljana, Slovenia
[2] Department of Physics, Faculty of Mathematics and Physics, and Institute of Biophysics, School of Medicine, University of Ljubljana, SI-1000 Ljubljana, Slovenia
[3] Department of Theoretical Physics, J Stefan Institute, SI-1000 Ljubljana, Slovenia

Received 19 October 2009, in final form 8 December 2009
Published 30 September 2010
Online at stacks.iop.org/JPhysCM/22/414102

Abstract

We present a mean-field theory for charged polymer chains in an external electrostatic field in the *weak* and *strong* coupling limits. We apply the theory to describe the statistical mechanics of flexible polyelectrolyte chains in a hexagonal columnar lattice of stiff cylindrical macroions, such as DNA, in a bathing solution of a uni-univalent salt (e.g. NaCl). The salt effects are first described in the Debye–Hückel framework. This yields the macroion electrostatic field in the screened Coulomb form, which we take to represent the mean field into which the chains are immersed. We introduce the Green's function for the polyelectrolyte chains and derive the corresponding Edwards equation which we solve numerically in the Wigner–Seitz cylindrical cell using the *ground state dominance ansatz*. The solutions indicate the presence of polyelectrolyte bridging, which results in a like-charge attraction between stiff macroions. Then we reformulate the Edwards theory for the strong coupling case and use the standard Poisson–Boltzmann picture to describe the salt solution. We begin with the free energy which we minimize to obtain the Euler–Lagrange equations. The solutions yield self-consistently determined monomer density and electrostatic fields. We furthermore calculate the free energy density as well as the total osmotic pressure in the system. We again show that bridging implicates like-charge attractions of entropic origin between stiff cylindrical macroions. By analyzing the osmotic pressure we demonstrate that, in certain parts of the parameter space, a phase transition occurs between two phases of the same hexagonal symmetry.

(Some figures in this article are in colour only in the electronic version)

1. Introduction

Systems composed of flexible polyelectrolytes in the background of an ordered macromolecular phase, as, for example, seen in the case of polyplexes, have been attracting a lot of theoretical and experimental attention in recent decades due to their numerous technological and medical applications [1]. Polyion–macroion interactions have been shown to play an important role in DNA self-assembly behavior [2–5], DNA packing in chromatin [6] and within viral capsids [7]. In all these cases the poly-counterions confer attractive interactions between stiffer DNA molecules that usually condense into an ordered phase with locally hexagonal symmetry.

The DNA condensation mechanisms in such systems are determined at least to some extent [3] by electrostatic and entropic free energy terms that we can successfully study using mean-field theories. Experimentally these systems have been studied intensely using a wide range of methods ranging from osmotic stress coupled to x-ray density determination [8] and light scattering [3, 4], to AFM single-molecule studies [9]. Several experiments have confirmed the existence of high density columnar DNA mesophases with hexagonal symmetry [8, 10–14].

 © 2010 IOP Publishing Ltd Printed in the UK & the USA

In a recent paper DeRouchey and co-workers investigated in detail the phase behavior of a columnar DNA phase using synchrotron small-angle x-ray scattering (SAXS) [8]. They report on a discontinuous phase transition from a compact hexagonal crystalline phase to loose bundles and finally to an isotropic phase with increasing salt concentration. Their free energy model describes polyelectrolytes as rigid rods which do not, as they themselves already point out, suit the experimental situations in all respects. In the present paper we thus concentrate on the opposite limit of flexible polyelectrolytes in order to supplement the calculation of polyelectrolyte-mediated interactions presented in [8]. Our approach is based on the mean-field formulation of the statistical mechanics of flexible polyelectrolyte chains in external electrostatic fields introduced before [15]. The results of this theory applied to an array of cylindrical macroions with hexagonal symmetry show that competition between electrostatic and entropic contributions to free energy can lead to a discontinuous phase transition in systems such as the one observed in [8] driven primarily by polyelectrolyte bridging between stiff (DNA) macromolecules.

Polyelectrolyte bridging refers to a situation where part of the same polyelectrolyte chain is adsorbed to one cylindrical macroion and the rest to a neighboring cylindrical macroion, pulling them together via the entropic effects of the connectivity of the chain. (For a detailed account and a complete list of references on the polyelectrolyte bridging interaction, see [16, 17].) The bridging interaction is thus strictly attractive.

In what follows we formulate a mean-field theory of flexible polyelectrolytes in the electrostatic field of oppositely charged orientationally and positionally ordered rod-like macroions in two distinct limits: first of all we treat the electrostatic field of rod-like macroions as completely decoupled from the local polyelectrolyte, which leads us to a formulation of the *weak coupling* model. Later on, by self-consistently including the effect of the local polyelectrolyte density on the mean electrostatic field in the system, we formulate the *strong coupling* model of interactions in this system. We analyze the corresponding osmotic pressure and show that it can exhibit a non-monotonic dependence on the macroion density, possibly giving rise to a first-order transition between two phases of equal symmetry.

2. Model description: the weak coupling case

Our system consists of a hexagonal lattice of uniformly charged, infinitely long and stiff rod-like macroions, flexible polyelectrolyte (PE) chains and a uni-univalent salt solution into which PE chains and stiff macroions are immersed. The stiff rod macroion approximation is legitimate for all macroion–polyelectrolyte systems where the macroion persistence length is much larger than its radius and where macroion persistence length exceeds that of the polyelectrolyte by orders of magnitude. This holds, for example, in the case of a system with DNA macroions (with a radius of 1 nm and persistence length of 50 nm) and poly-lysine and poly-arginine polyelectrolyte chains with much smaller persistence length [8]. We hold the coupling between the polyelectrolyte density and the external electrostatic field to be weak in those cases where the external field dictates the shape of the PE density profiles, but not vice versa. In other words, in the weak coupling limit PE monomers have no impact on the external electrostatic field even though they are themselves charged. It is set only by the fixed charges on the macroions. This approximation clearly works only in the case where the PE chains are extremely weakly charged and should be viewed like a first-order perturbation theory on the complete electrostatic coupling [15] which is then treated appropriately on the strong coupling limit (see below).

We describe the macroion electrostatic field screened by salt ions on the Debye–Hückel level, corresponding to a linearized Poisson–Boltzmann theory, which yields the familiar form for the screened electrostatic potential of a cylindrical macroion $\phi(r) = A_0 K_0(\kappa r)$, where r is the off-axis separation from the cylindrical macroion and $K_0(\kappa r)$ is the modified Bessel function of the second kind. $A_0 = \frac{\mu e_0}{4\pi\epsilon\epsilon_0 k_B T} = \frac{\mu}{e_0}\frac{e}{e_0} l_B$ is the dimensionless interaction parameter, μ is the linear charge density of the cylindrical macroion defined as charge e per Kuhn's length b, $l_B = e^2/4\pi\epsilon\epsilon_0 k_B T$ is the standard Bjerrum length and κ stands for the inverse Debye screening length $\kappa = \lambda_D^{-1}$. e_0 is the unit charge and ϵ is the static permittivity of water.

The statistics of polyelectrolyte chain conformations in an external field is described by the standard polyelectrolyte Green function [18]:

$$G_N(\mathbf{r}', \mathbf{r}; \phi) = \int_{\mathbf{r}'}^{\mathbf{r}} \mathcal{D}\mathbf{r}(n) \mathrm{e}^{-\frac{3}{2b^2}\int_0^N \mathrm{d}n (\frac{\partial \mathbf{r}(n)}{\partial n})^2 - \beta e \int_0^N \mathrm{d}n\, \phi(\mathbf{r}(n))} \quad (1)$$

where the integral over n in the exponent runs along the contour of the PE chain of N monomers, b is the chain's Kuhn length while $\beta = 1/k_B T$ stands for the inverse thermal energy. The first term in the exponent describes the chain connectivity and entropy while the second one describes the Boltzmann weights of the chain in an external electrostatic potential ϕ. The notation $\int \mathcal{D}\mathbf{r}(n)$ stands for the functional integral over all possible polyelectrolyte chain conformations. The Green function of the PE chain of N monomers can be interpreted as the probability density that the chain's end-to-end vector $\mathbf{r}_{ee} = \mathbf{r}(N) - \mathbf{r}(0)$ will span the difference $\mathbf{r} - \mathbf{r}'$ or, which amounts to the same thing, as the probability density that a chain of N monomers has its last monomer at $\mathbf{r}$ provided its first monomer is at $\mathbf{r}'$. The polymer Green's function has to satisfy the Edwards equation [18, 19]:

$$-\frac{b^2}{6}\nabla^2 G_N + \beta e \phi G_N = -\frac{\partial G_N}{\partial N}. \quad (2)$$

Since the Edwards equation is formally analogous to the quantum Schrödinger equation, being Wick-rotated in the time domain, we can proceed by similar means to solve it. We define eigenfunctions ψ_k of the Edwards operator through

$$\left(-\frac{b^2}{6}\nabla^2 + \beta e \phi\right)\psi_k = \mathcal{E}_k \psi_k.$$

After performing an eigenfunction expansion of the Green's function $G_N(\mathbf{r}', \mathbf{r}) = b^3 \sum_k \psi_k^*(\mathbf{r}')\psi_k(\mathbf{r})\, e^{-N\mathcal{E}_k}$ and truncating

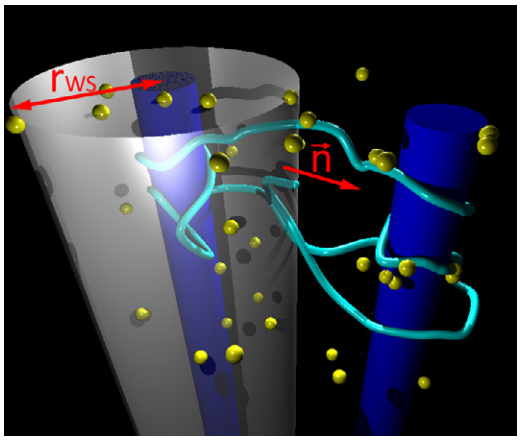

Figure 1. Schematic depiction of our model with its Wigner–Seitz cell. Cylindrical macroions in a columnar phase are shown as blue cylinders of radius a, electrolyte ions are depicted as yellow spheres, while the polyelectrolyte chain is green. The transparent cylinder represents the Wigner–Seitz cell with surface normal $\mathbf{n}$ and radius r_{WS}. The radius of the cylindrical macroions, a, is always taken as 1 nm.

the series after its first term—the *ground state dominance approximation* (GSDA) [18]—we obtain the following approximate relations for the Green's function and the free energy:

$$G_N(\mathbf{r}, \mathbf{r}') \simeq \psi_0^*(\mathbf{r})\psi_0(\mathbf{r}')\mathrm{e}^{-\mathcal{E}_0 N} \tag{3}$$

$$\mathcal{F} \simeq k_{\mathrm{B}}TN\mathcal{E}_0. \tag{4}$$

It is then straightforward to show that the polyelectrolyte monomer density may be expressed as [19]

$$\rho(\mathbf{r}) = N\psi_0^2(\mathbf{r}). \tag{5}$$

Note that the ground state dominance approximation only makes sense for chains that are much longer than their persistence lengths [20]. We feel no need to go deeper into the mathematical specifics of the GSDA since this has already been adequately done elsewhere [15].

We solve the Edwards equation (2) describing our system in a polyelectrolyte and salt-filled cylindrical Wigner–Seitz (WS) unit cell surrounding a lattice macroion placed in the cell's axis of symmetry as shown in figure 1.

Each cell is, by assumption, electroneutral and the coupling between them is provided solely by the appropriate boundary conditions for the mean electrostatic field. The WS cell approach thus effectively decouples the partition function of the entire system into a product of disjoint single macroion factors, thus reformulating a many-body problem in the mean-field framework. This approach should work fine if the polyelectrolyte chain spans only a few WS cells, which is what we assume here. If a single polyelectrolyte chain connects many different macroions a collective approach is in order, as formulated in [21].

In cylindrical geometry we may only keep the radial part of the Laplace operator in the Edwards equation since our system is translationally invariant along the principal axis of the Wigner–Seitz cell. The Edwards equation thus assumes the form (see [21])

$$\psi_0''(r) + \frac{1}{r}\psi_0'(r) + \frac{6}{b^2}(A_0K_0(\kappa r) + \mathcal{E}_0)\psi_0(r) = 0. \tag{6}$$

$\mathcal{E}_0$ is the ground state energy eigenvalue of the Edwards operator $-\frac{b^2}{6}\nabla^2 + \beta e\phi$.

The boundary conditions pertaining to equation (6) in the Wigner–Seitz cell are as follows. We simulate the hexagonal packing symmetry of the macroions by demanding that the normal derivative of the density field ψ_0 should vanish on the surface of the Wigner–Seitz cell:

$$\left.\frac{\partial\psi_0}{\partial\mathbf{n}}\right|_{r=r_{\mathrm{WS}}} = 0.$$

To fix the number of PE chains in the system the ground state eigenfunction must be normalized: $\int \mathrm{d}\mathbf{r}\,\psi_0^2(\mathbf{r}) = 1$. Furthermore we require that the PE chain is not allowed to penetrate into the macroion, thus setting the PE chain density on the macroion surface to zero:

$$\psi_0|_{r=a} = 0.$$

The surface charge density of the macroion is assumed to be $\sigma = \sigma_{\mathrm{DNA}} \approx 1e_0\ \mathrm{nm}^{-2}$, corresponding approximately to the surface charge density of DNA with a radius of $a = 1$ nm, carrying a linear charge density $\mu = 1e_0/1.7$ Å.

2.1. Solutions of the Edwards equation

We solved equation (6) numerically in a cylindrical Wigner–Seitz cell using a combination of standard shooting and minimization algorithms and we now proceed to the results. Figure 2 shows the polyelectrolyte density profile $\rho(w) \sim \psi^2(w)$ as a function of reduced radial coordinate $w = \kappa r$ for different values of κ. The value of the dimensionless interaction parameter is taken as $A_0 = 10$. The monomer density profile clearly exhibits a transition from depleted (monotonic profiles) to surface bound states (non-monotonic profiles) as we reduce the inverse screening length κ.

Surface bound states indicate the presence of polyelectrolyte bridging [16] which grows stronger as we reduce the concentration of the uni-univalent electrolyte in the cell. This is due to the fact that, at short screening lengths, the effect of electrostatics is diminished, the system is effectively discharged and polyelectrolyte adsorption to charged macroions cannot be the dominant mechanism of the free energy minimization. In this case free energy is minimized through enhanced entropic steric effects which prefer the chain to be as far from the macroion surface as possible.

A similar effect occurs when we fix the values of parameters A_0 and κ and observe the PE monomer density profiles while increasing the cell's radius, which corresponds to the changes in the concentration of the macroions. At high macroion concentrations the dominant mechanism of free energy minimization is entropy maximization which leads to a surface-depleted regime where the chain is mostly concentrated at the periphery of the WS cell, i.e. in the space between the macroions. At lower macroion concentrations the

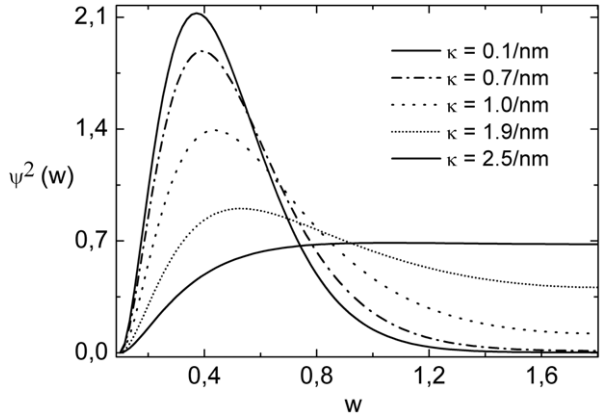

Figure 2. Polyelectrolyte density profile $\rho(w) \sim \psi^2(w)$ as a function of reduced radial coordinate $w = \kappa r$ for different values of κ. The value of the dimensionless interaction parameter is $A_0 = 10$, corresponding to DNA. The profile clearly exhibits a transition from depleted to surface bound states as we reduce the inverse screening length κ. Surface bound states indicate the presence of bridging interactions which grow stronger as we reduce the molarity of salt.

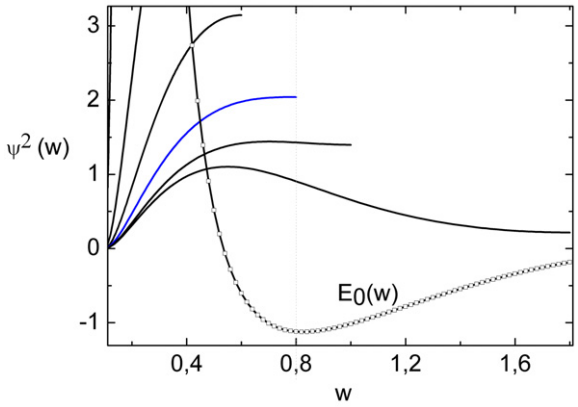

Figure 3. Polyelectrolyte monomer density profiles and ground state energy eigenvalues at different cell diameters for fixed parameter values $A_0 = 3$ and $\kappa = 0.1$ nm^{-1}. There is no bridging present at high macroion concentrations (corresponding to small WS cell diameter) but if the macroion density is decreased so that the corresponding WS cell diameter is $w_{\mathrm{WS}} > 0.8$ (dotted line) the monomer density distribution becomes bimodal and the eigenenergy curve goes through a minimum (vertical dotted line), indicating the presence of attractive bridging interactions.

electrostatic interactions become strong enough to significantly increase the monomer concentration close to the macroion surface which leads to attractive bridging interactions between neighboring macroions. This is shown in figure 3 which depicts monomer density profiles and ground state energy eigenvalues at different cell diameters for fixed parameter values $A_0 = 3$ and $\kappa = 0.1$ nm^{-1}. The cell diameter variations have a pronounced effect on the density profiles which are monomodal (implying that no bridging is present) up until we increase the dimensionless diameter over the 'critical' value of $w_{\mathrm{WS}} \approx 0.8$. At that point the monomer density distributions become bimodal and the free energy curve goes through a minimum. Since the forces between macroions are related to polyelectrolyte osmotic pressure

$$p^* = -\left(\frac{\partial \mathcal{F}(w)}{\partial V}\right)_{w=w_{\mathrm{WS}}} = -k_{\mathrm{B}}TN\frac{\partial E_0(w_{\mathrm{WS}})}{\partial V} \qquad (7)$$

non-monotonic free energy behavior, such as the one shown in figure 3, indicates the presence of attractive bridging interactions due to the interplay between the chain entropy and electrostatic interactions between the chain and the charged macroion.

3. Strong coupling case: self-consistent field theory for chains in cylindrical cells

The theory presented above does not take into account the fact that polyelectrolyte monomers are themselves charged and as such modify the electrostatic field in the WS cell as well. In what follows we reformulate the theory to describe cases where this coupling is too large to be ignored: in our description we remain close to the Poisson–Boltzmann theory which we generalize to include polyelectrolyte chain contributions to the electrostatic field in a self-consistent manner. We arrive at a new set of self-consistent field equations which are solved numerically in different regions of the parameter space. The solutions indicate the presence of a discontinuous phase transition which was unobtainable within the framework of the weak coupling theory. In our brief outline of the derivation of the self-consistent field equations we follow closely the derivation for planar geometries thoroughly presented in [15].

The polyelectrolyte chain is again described using the Edwards model in the ground state dominance approximation. The contour length of the chain is Nb, where N is the number of monomers of Kuhn length b. In addition the total number of chains in the system is assumed to be $\mathcal{N}$. They are all identical. All electrostatic interactions in the system are mediated via a Coulomb kernel $u(\mathbf{r}, \mathbf{r}') = (1/4\pi\epsilon\epsilon_0)|\mathbf{r} - \mathbf{r}'|^{-1}$. The system is described as monodisperse and we assume a homogeneous linear charge distribution along each polyelectrolyte chain and a homogeneous surface charge density σ on all columnar macroions. The Hamiltonian of the system then is

$$\begin{aligned}\beta\mathcal{H} = {} & \frac{3}{2b^2}\sum_{\alpha=1}^{\mathcal{N}}\int_0^N \mathrm{d}n\left(\frac{\partial \mathbf{r}^\alpha(n)}{\partial n}\right)^2 \\ & + \frac{\beta}{2}\int\int \mathrm{d}\mathbf{r}\,\mathrm{d}\mathbf{r}'\,\rho(\mathbf{r})\rho(\mathbf{r}')u(\mathbf{r},\mathbf{r}') \\ & + \beta\int \mathrm{d}\mathbf{r}\,\rho(\mathbf{r})\phi(\mathbf{r}),\end{aligned} \qquad (8)$$

where α runs over all the chains in the system, $\mathbf{r}^\alpha(n)$ is the αth chain contour parameterized with the parameter n, $\rho(\mathbf{r})$ is the density of all volume charges (electrolytes and polyelectrolytes) in the system and ϕ is the electrostatic potential due to macroion surface charges. The first term in Hamiltonian equation (8) describes the chain entropic contribution due to its connectivity, the second term represents all the electrostatic interactions between volume charges while the third term stands for electrostatic interactions of volume charges with the macroion electrostatic field. To get rid of

the nonlocal character of the above Hamiltonian we perform a Hubbard–Stratonovich transformation. We may then formally proceed to write the system partition function in the following useful form (for a detailed derivation see [15]):

$$\Xi = \Delta(\beta) \int \mathcal{D}\phi \mathrm{e}^{-\beta S_\phi}, \tag{9}$$

where $\int \mathcal{D}\phi$ is a functional integral measure over fluctuating electrostatic fields ϕ, $\Delta(\beta) = (2\pi)^{N/2}\sqrt{\det[\beta u^{-1}(\mathbf{r},\mathbf{r})]}$ and the action functional S_ϕ is

$$S_\phi = \mathcal{H}_{\mathrm{PB}}[\mathrm{i}\phi] - k_\mathrm{B}T\mathcal{N}\ln\left(\int\int G_N(\mathbf{r},\,\mathbf{r}';\phi)\mathrm{d}^3\mathbf{r}\,\mathrm{d}^3\mathbf{r}'\right). \tag{10}$$

The first term in equation (10) is a Wick-rotated version of the Poisson–Boltzmann free energy [15] and

$$\mathcal{H}_{\mathrm{PB}}[\phi] = 2k_\mathrm{B}Tn_0\int \mathrm{d}\mathbf{r}\cosh(\beta e_0\phi(\mathbf{r})) + \oint \mathrm{d}\mathbf{s}\,\sigma\phi(\mathbf{s}) - \frac{\epsilon\epsilon_0}{2}\int \mathrm{d}\mathbf{r}(\nabla\phi(\mathbf{r}))^2 \tag{11}$$

is the usual Poisson–Boltzmann Hamiltonian with n_0 as the electrolyte number density. $G_N(\mathbf{r},\,\mathbf{r}';\phi)$ is again the polyelectrolyte Green function defined in equation (1). There are several approximate approaches to calculating the free energy from the partition function (9) and we use one of them, the so-called *saddle point approximation*. We approximate the functional integral in (9) by its largest contribution which corresponds to the exponent of the action functional calculated at its saddle point S_φ^{SCF}, namely

$$\int \mathcal{D}\phi\, e^{-\beta S_\phi} \simeq \exp[-\beta S_\varphi^{\mathrm{SCF}}].$$

This leads to the consideration of the saddle point configurations of the fluctuating electrostatic field, φ, defined as solutions of

$$\delta S_\phi/\delta\varphi(\mathbf{r})|_{\phi=\varphi} = 0. \tag{12}$$

As is well known from the polymer theory the self-consistent field calculation coincides with the saddle point approximation. In fact, they represent the same approximation and its ramifications have been studied in detail [22].

Along with the Edwards equation (2) the saddle point equation yields the following system of self-consistent field (SCF) equations for the mean electrostatic field φ and the polymer density field ψ in the ground state dominance approximation equation (5)

$$\epsilon\epsilon_0\nabla_\perp^2\varphi(\mathbf{r}) - 2k_\mathrm{B}Tn_0\sinh[\beta e_0\varphi(\mathbf{r})] - e\mathcal{N}N|\psi(\mathbf{r})|^2 = 0 \tag{13}$$

$$-\frac{l^2}{6}\nabla_\perp^2\psi(\mathbf{r}) + \beta e\varphi(\mathbf{r})\psi(\mathbf{r}) - \mathcal{E}_0\psi(\mathbf{r}) = 0. \tag{14}$$

Here e again stands for the net charge on each monomer and $\nabla_\perp^2 = r^{-1}(\partial/\partial r)(r\partial/\partial r)$ for the radial part of the Laplace operator. It is straightforward to see that, in the absence of polyelectrolyte, equation (13) simplifies to the standard Poisson–Boltzmann equation for the uni-univalent salt, while equation (14) has the form of the Edwards equation where the electrostatic potential $\varphi(\mathbf{r})$ has yet to be determined self-consistently with the polyelectrolyte density field $\psi(\mathbf{r})$.

The boundary conditions to equations (13) and (14) are as follows. To simulate the hexagonally packed macroions we stipulate that radial derivatives of the electrostatic and PE density fields vanish at the Wigner–Seitz cell surface, so that

$$\frac{\partial\varphi}{\partial\mathbf{n}}(r = r_{\mathrm{WS}}) = 0 \qquad \text{and} \qquad \frac{\partial\psi}{\partial\mathbf{n}}(r = r_{\mathrm{WS}}) = 0.$$

Since the chain cannot penetrate into the macroion, PE chain density on the macroion surface must also vanish, leading to

$$\psi(r = a) = 0.$$

In addition, in order to ensure the electroneutrality of each cell the following standard boundary condition must hold on the macroion surface of surface charge density σ:

$$-\epsilon\epsilon_0\frac{\partial\varphi}{\partial\mathbf{n}}(r = a) = \sigma.$$

To fix the number of chains in each cell, we must make sure the PE density field solutions to equations (13) and (14) are properly normalized, namely that $\int \mathrm{d}\mathbf{r}|\psi(\mathbf{r})|^2 = 1$.

3.1. Solutions of the SCF equations

Before we set out to solve the SCF equations numerically it is useful to rewrite them in dimensionless form. Without any loss of generality we may assume in what follows that $e = e_0$. We now introduce dimensionless distance $w = \lambda_\mathrm{D}^{-1}r = \kappa r$, dimensionless macroion surface charge density $\beta e_0\lambda_\mathrm{D}\sigma/\epsilon\epsilon_0$ and dimensionless parameter $\lambda^{*2} = (\beta e_0^2/\epsilon\epsilon_0)\mathcal{N}(N/S)\lambda_\mathrm{D}$, which measures the ratio between the number of PE chains and the amount of salt in the cell. At room temperature we can calculate the dimensionless macroion surface charge density to be $\beta e_0\lambda_\mathrm{D}\sigma/\epsilon\epsilon_0 \approx 9\ \mathrm{nm}\cdot\lambda_\mathrm{D}(\sigma/e_0)$, assuming the static permittivity of water to be $\epsilon = 80$. Following the experimental data [23] we have set Kuhn's length of the polyelectrolyte to 1 nm. Introducing furthermore the dimensionless electrostatic field $\varphi \to \beta e_0\varphi$, we can rewrite equations (13) and (14) in the dimensionless form:

$$\frac{\mathrm{d}^2\psi}{\mathrm{d}w^2} + \frac{1}{w}\frac{\mathrm{d}\psi}{\mathrm{d}w} + 6(\lambda_\mathrm{D}/b)^2(\mathcal{E}_0 - \varphi)\psi = 0 \tag{15}$$

$$\frac{\mathrm{d}^2\varphi}{\mathrm{d}w^2} + \frac{1}{w}\frac{\mathrm{d}\varphi}{\mathrm{d}w} - \sinh\varphi + \lambda^{*2}\psi^2 = 0. \tag{16}$$

The transformations of the appropriate boundary conditions are straightforward and we do not state them explicitly at this point.

In what follows we obtain the solutions of the SCF equations (15) and (16) numerically using a combination of iterative shooting and minimization methods. Figure 4 shows polyelectrolyte density profiles in cylindric Wigner–Seitz cells for different screening lengths λ_D at parameter values $\sigma = 6\sigma_{\mathrm{DNA}}$, $\lambda_\mathrm{D} = 0.7{:}0.2{:}1.3$ nm and $\lambda^{*2} = 1$. The macroion rod is not depicted in the images but is located in the axis of symmetry of each density profile. Since this is the case of extremely high macroion surface charge density the transition

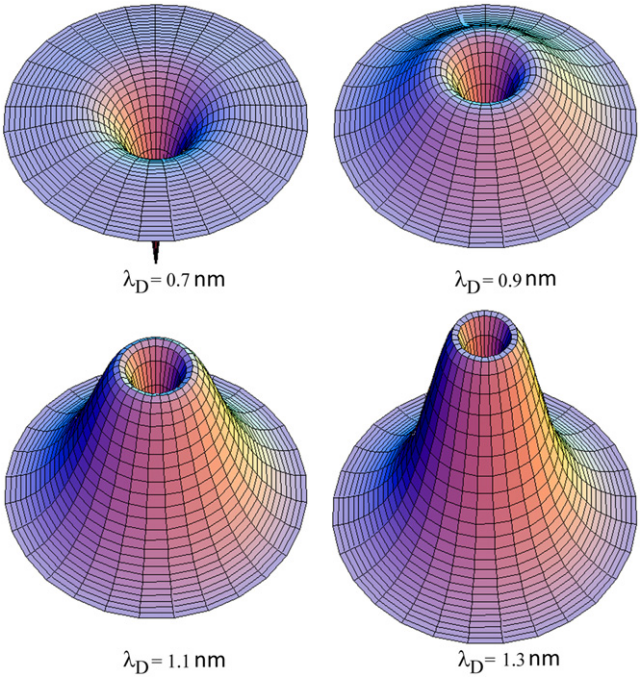

Figure 4. Polyelectrolyte density profiles $\rho(w) \sim \psi^2(w)$ in cylindrical Wigner–Seitz cells for different screening lengths λ_D at parameter values $\sigma = 6\sigma_{DNA}$, $\lambda_D = 0.7{:}0.2{:}1.3$ nm and $\lambda^{*2} = 1$. The macroion rod is not depicted in the images but is located in the axis of symmetry of each density profile. As we lower the salt content in each cell the surface bound states become more explicit and the maximum of the monomer density distribution shifts closer to the macroion surface.

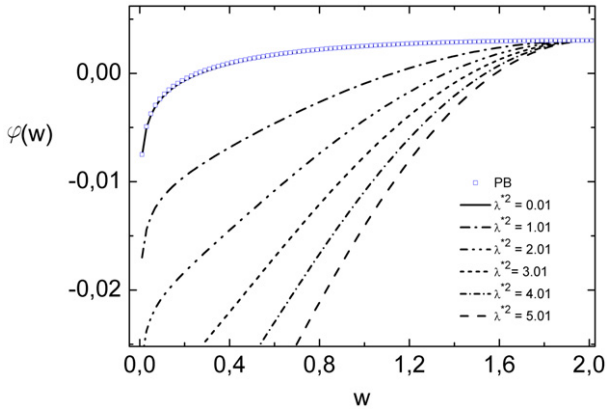

Figure 5. Electrostatic field solutions of the complete SCF system (lines) alongside with numerical solution to the cylindrical Poisson–Boltzmann equation (squares) at parameters $\sigma = 0.1\sigma_{DNA}$, $\lambda_D = 0.26$ nm and $\lambda^{*2} = 0.01{:}1{:}5.01$. As expected, both theories yield the same results in the absence of polyelectrolytes (where $\lambda^{*2} \sim 0$).

from depleted (profile at $\lambda_D = 0.7$ nm) to surface bound states (profiles at $\lambda_D = 0.9$, 1.1 and 1.3 nm) is very clear.

Self-consistent electrostatic field solutions in the system are shown in figure 5 along with a numerical solution of the cylindrical Poisson–Boltzmann equation without the polyelectrolyte at parameter values $\sigma = 0.1\sigma_{DNA}$, $\lambda_D = 0.26$ nm and $\lambda^{*2} = 0.01{:}1{:}5.01$. We have varied the polyelectrolyte content λ^{*2} in the cell from 0.01 to 5.01 but held the macroion charge density and salt concentration fixed. Low values of λ^{*2} mean low polyelectrolyte densities while high values of λ^{*2} mean high densities. The blue squares in figure 5 show the Poisson–Boltzmann electrostatic field solutions while black lines represent φ-field solutions to the full SCF system. Since Poisson–Boltzmann theory is the limiting case of the self-consistent field theory for low polyelectrolyte densities, we expect the two solutions to coincide in the low polyelectrolyte density regime ($\lambda^{*2} \sim 0$), as they in fact do. Figure 5 shows that Poisson–Boltzmann theory gives quantitatively correct electrostatic field profiles only as long as the concentration of polyelectrolytes is low enough ($\lambda^{*2} \sim 0.01$) while at higher densities the differences between the two theories grow in favor of the self-consistent field approach.

4. Osmotic pressure

The interaction between like-charged macroions on different lattice sites has two components [16]: (i) counterion and salt-screened electrostatic repulsion and (ii) attractive polyelectrolyte-mediated bridging interactions of entropic origin. We show below that the competition between these mechanisms leads to non-monotonic behavior of free energy and osmotic pressure.

Using the saddle point approximation we can calculate the ground state eigenenergy $\mathcal{E}_0$ and the fields φ and ψ and then obtain the system's free energy as the logarithm of the partition function in the form

$$\mathcal{F}(w) = -k_B T \ln \Xi = k_B T \mathcal{N}(N/S)\mathcal{E}_0(w) + \mathcal{H}_{PB}[\varphi(\mathbf{r})] \quad (17)$$

where $\mathcal{H}_{PB}[\varphi(\mathbf{r})]$ is the standard Poisson–Boltzmann Hamiltonian defined in (11). The dimensionless osmotic pressure is then given by $p^* = (e_0\lambda_D)^2/(\epsilon\epsilon_0(k_B T)^2) \cdot p$, where p is the standard osmotic pressure given by the negative derivative of the free energy with respect to the volume of the Wigner–Seitz cell.

Figure 6 shows osmotic pressure profiles for three different macroion surface charges, two different Debye screening lengths and fixed polyelectrolyte density. Salt concentration obviously has a profound impact on the sign of the forces between the macroions. At high salt concentrations the forces between the macroions stay repulsive for all distances (see the uppermost curve on figure 6). At low concentrations the pressure profiles for $\lambda_D = 1.21$ nm are all non-monotonic with long range negative tails implying attractive bridging forces of order 10^{-2} pN nm^{-2} = 10 atm between like-charged macroions.

In certain regions of the parameter space we encounter osmotic pressure profiles of van der Waals type, indicating a discontinuous phase transition between phases of equal symmetry. We have analyzed these pressure profiles using the Maxwell construction and determined the spinodal and the coexistence regions in the phase diagrams by calculating the dependence of the critical pressure on the macroion surface charge density. The critical pressure is defined via the critical iso-ionic strength line that separates the regime of monotonic

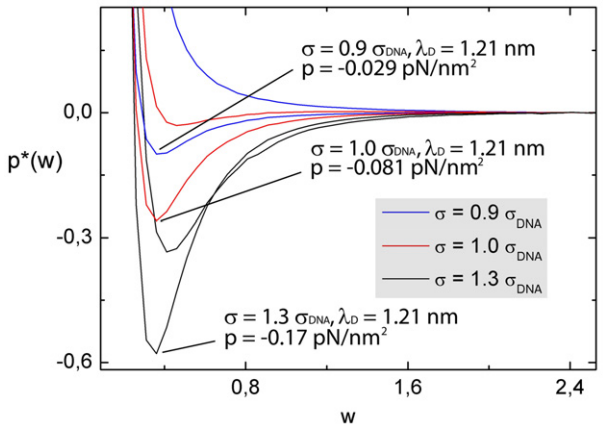

Figure 6. Osmotic pressures at three different macroion surface charges ($\sigma = 0.9, 1, 1.3\ \sigma_{\mathrm{DNA}}$, see legend), two different Debye screening lengths ($\lambda_{\mathrm{D}} = 0.91$ nm (top curve at each σ) and $\lambda_{\mathrm{D}} = 1.21$ nm (bottom curve at each σ)) and fixed polyelectrolyte density ($\lambda^{*2} = 0.35$). Pressure profiles for $\lambda_{\mathrm{D}} = 1.21$ nm are all non-monotonic with long range negative tails implying attractive bridging forces of order 10^{-2} pN nm^{-2} = 10 atm between like-charged macroions. The magnitude of the attractive bridging forces is stated for each macroion charge density at $\lambda_{\mathrm{D}} = 1.21$ nm.

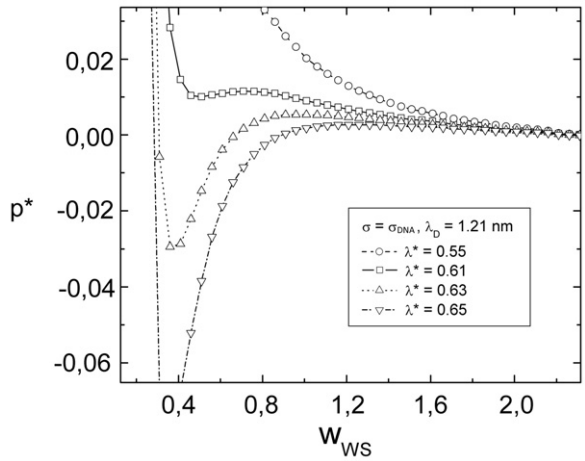

Figure 7. Osmotic pressure in the vicinity of a discontinuous phase transition at fixed parameters $\sigma = \sigma_{\mathrm{DNA}}$, $\lambda_{\mathrm{D}} = 1.21$ and at various values of λ^{*2}. From top to bottom the values of λ^{*2} are 0.65, 0.63, 0.61 and 0.55. At high macroion and polyelectrolyte densities (uppermost curve at $\lambda^{*2} = 0.65$) the system is dominated by steric polyelectrolyte repulsion while at lower densities a hexagonal crystalline–line hexatic phase transition occurs which allows for enhanced bridging interactions, yielding like-charge macroion attractions.

osmotic pressures from the one with a van der Waals type loop behavior in complete analogy with the van der Waals theory of first-order transitions. An example of a van der Walls-like iso-ionic strength curve (a curve along constant values of λ_{D}) is seen in figure 7 showing osmotic pressure in the vicinity of a phase transition at fixed parameters $\sigma = \sigma_{\mathrm{DNA}}$, $\lambda_{\mathrm{D}} = 1.21$ and at various values of λ^{*2}. From top to bottom the values of λ^{*2} are 0.65, 0.63, 0.61 and 0.55. Note that at fixed Debye length higher values of λ^{*2} signify higher densities of polyelectrolyte. The two phases in this transition, corresponding to the same packing symmetry of the macromolecules, could correspond (possibly) to the hexagonal and line hexatic phases as observed in [24]. This identification is, of course, very tentative.

Figure 7 indicates that at small macroion interaxial spacings or at high polyelectrolyte densities (the uppermost curve with $\lambda^{*2} = 0.65$) the largest contribution to the osmotic pressure stems from the steric confinement of the PE chains between the macroions. As we lower the polyelectrolyte densities (as λ^{*2} varies from 0.65 to 0.55) we observe a coexistence region of tightly packed and loosely packed phases determined by the Maxwell construction for $\lambda^{*2} \lesssim 0.59$. A tightly packed structure could possibly correspond to a hexagonal crystalline phase and a loosely packed structure to a line hexatic phase seen in DNA in a different context [24]. Both phases are schematically presented as an inset to figure 8 which shows outlines of coexistence curves obtained from Maxwell constructions on a set of van der Waals-like iso-ionic pressure–volume curves for different values of macroion surface charge density. Illustrations of the two phases of equal symmetry are added to their respective regions of phase space.

It is clear from figure 8 that macroion surface charge density has a profound impact on the phase diagram. The critical point of the coexistence curve at $\sigma = 0.9\sigma_{\mathrm{DNA}}$ (lowermost curve square symbol) is located at a much lower

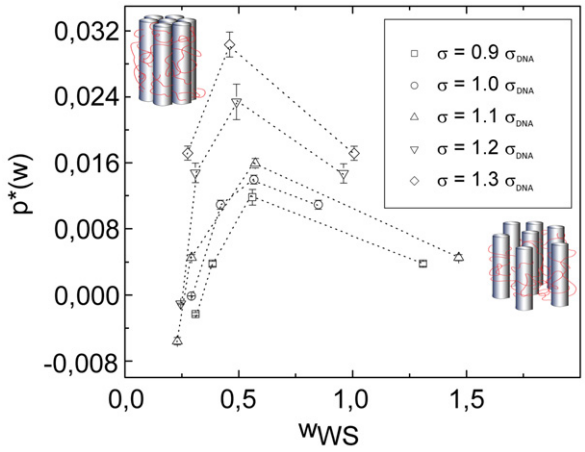

Figure 8. Outlines of calculated coexistence curves obtained from Maxwell constructions on a set of van der Waals-like iso-ionic strength pressure–volume curves for different values of macroion surface charge density. We have varied surface charge density from $\sigma = 0.9\sigma_{\mathrm{DNA}}$ to $\sigma = 1.3\sigma_{\mathrm{DNA}}$ with step 0.1 σ_{DNA} at fixed Debye length $\lambda_{\mathrm{D}} = 1.21$ nm. Dotted lines serve strictly as guides to the eyes.

osmotic pressure than the one at $\sigma = 1.3\sigma_{\mathrm{DNA}}$ (uppermost curve with diamond symbol). This tells us that at lower macroion charge densities entropic contributions can be neglected in comparison to steric interactions at much lower pressures. At higher macroion charge densities bridging, which arises from electrostatic adsorption of the chain to the macroion surface, remains present also for pressures which would, at lower macroion charge densities, already enforce steric domination—yielding monotonic repulsive forces. We can extract a similar conclusion from dimensionless

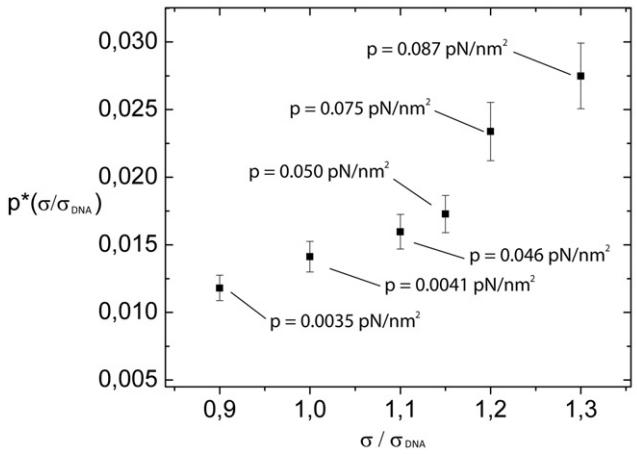

Figure 9. Dimensionless critical pressure dependence on the macroion charge density $p_c^*(\sigma/\sigma_{DNA})$. We show calculated critical pressures for surface charge densities 0.9, 1.0, 1.1, 1.15, 1.20 and 1.30 σ_{DNA}. We show also values for pressures $p = \epsilon\epsilon_0(k_BT)^2p^*/(e_0\lambda_D)^2$. Error bars are due to the fact that during calculations it was impossible to 'hit' exactly the critical parameters during the shooting algorithm so we were forced to estimate critical values from numerically neighboring solutions.

critical pressure dependence on the macroion charge density $p_c^*(\sigma/\sigma_{DNA})$ shown in figure 9. The critical iso-ionic strength line separates the monotonic pressure–volume curves from those showing a van der Waals loop. In figure 9 we show calculated critical pressures for surface charge densities 0.9, 1.0, 1.1, 1.15, 1.20 and 1.30 σ_{DNA}. We see that the dimensional critical pressure $p = \epsilon\epsilon_0(k_BT)^2p^*/(e_0\lambda_D)^2$ monotonically rises for more than 0.085 pN nm^{-2} as we increase the macroion charge density from $0.9\sigma_{DNA}$ to $1.3\sigma_{DNA}$.

Note that, due to a relatively minor change in surface charge density, the critical pressure in the system increases by almost two orders of magnitude. This implies yet again that the DNA molecule—highly charged as it is—may be especially suitable for self-assembly mechanisms that are due to polyelectrolyte bridging interactions.

5. Discussion

Measurements and theoretical descriptions of the bridging interactions in macroion–polyelectrolyte complexes all indicate that electrostatic approaches that disregard polyelectrolyte configurational entropic effects are probably insufficient. It is these entropic contributions to free energy that give rise to attractive bridging interactions between like-charged macroions while electrostatic contributions—if treated in the self-consistent field framework—invariably give rise to longer range Poisson–Boltzmann repulsions. The combination of these short range bridging attractions and longer ranged electrostatic repulsions can give rise to a first-order transition between two macroion phases of equal symmetry but different densities.

Though our calculation was not designed specifically for any particular system composed of stiff macroions and flexible PE chains the behavior that we observe can be in many aspects connected with the observed salient features of the DNA–PE mixtures that have been recently extensively studied [3, 4, 8]. We could thus argue that at least some part of the attractive interactions responsible for self-assembly in these systems is due exactly to polyelectrolyte bridging mechanisms.

The theoretical approaches described in this paper have several well-known drawbacks. First of all, any mean-field or self-consistent field approaches completely disregard electrostatic fluctuation and correlation effects [22] which can lead to sign reversal and oscillatory force behavior for higher valence counterions. Our analysis also does not include polydispersity or intra-chain charge–charge correlations which result in electrostatic stiffening of the chain. The ground state dominance approach has limited our investigation to chains with contour lengths much longer than their persistence length, thereby neglecting all free tail effects that have been theoretically investigated elsewhere. We furthermore assumed soft electrostatic adsorption of chains and ignored the possibility of polyelectrolyte grafting or specific adsorption to the surface of macroions. This assumption invariably yields a polyelectrolyte depleted zone in the vicinity of the macroion which obviously is not always the case, e.g. in the polyelectrolyte brushes.

In the weak coupling limit we employed a linearized Debye–Hückel version of the Poisson–Boltzmann theory which is by definition unable to describe any nonlinear effects. Our work does, however, consist of the first full numerical solution of the Edwards equation in a cylindrical Wigner–Seitz cell in the presence of salt and macroions whereas analytical approximations and variational approaches in similar systems have already been employed by one of the authors.

In the strong coupling limit we have self-consistently coupled the nonlinearized Poisson–Boltzmann theory for bulk electrolytes with the Edwards functional integral description of polyelectrolyte density on a hexagonal DNA lattice. We have solved the self-consistent field equations numerically and demonstrated a salt-induced phase transition between hexagonal and line hexatic DNA phases.

Further work should be done by including Flory-type steric ψ^4 terms to free energy to describe intra-and inter-chain excluded-volume interactions.

Acknowledgments

RP would like to acknowledge the financial support by the Slovenian Research Agency under contract no. P1-0055 (Biophysics of Polymers, Membranes, Gels, Colloids and Cells) and J1-0908 (Active media nanoactuators with dispersion forces).

References

[1] Kabanov A V, Felgner P and Seymour L W (ed) 1998 *Self-Assembling Complexes for Gene Delivery* (New Jersey: Wiley)
[2] De Rouchey J and Rau D C 2009 in preparation
[3] Toma A C, de Frutos M, Livolant F and Raspaud E 2009 *Biomacromolecules* at press
[4] Korolev N, Berezhnoy N V, Eom K D, Tam J P and Nordenskiold L 2009 *Nucl. Acids Res.* at press
[5] Koltover I, Salditt T and Safinya C R 1999 *Biophys. J.* **77** 915
[6] Schiessel H 2003 *J. Phys.: Condens. Matter* **15** 699

[7] Leforestier A and Livolant F 2009 *Proc. Natl Acad. Sci.* **106** 9157
[8] DeRouchey J, Netz R R and Raedler J O 2005 *Eur. Phys. J. E Soft Matter* **16** 17
[9] Minko S and Roiter Y 2005 *Curr. Opin. Colloid Interface Sci.* **10** 9
[10] Koltover I, Salditt T, Rädler J and Safinya C R 1998 *Science* **281** 78
[11] Podgornik R, Strey H H, Gawrisch K, Rau D C, Rupprecht A and Parsegian V A 1996 *Proc. Natl Acad. Sci.* **93** 4261
[12] Strey H H, Parsegian V A and Podgornik R 1997 *Phys. Rev. Lett.* **78** 895
[13] Podgornik R, Strey H H and Parsegian V A 1998 *Curr. Opin. Colloid Interface Sci.* **3** 534
[14] Ewert K K, Evans H M, Zidovska A, Bouxsein N F, Ahmad A and Safinya C R 2006 *J. Am. Chem. Soc.* **128** 3998
[15] Podgornik R 1992 *J. Phys. Chem.* **96** 884
[16] Podgornik R 2004 *J. Polym. Sci.* B **42** 3539
[17] Podgornik R and Ličer M 2006 *Curr. Opin. Colloid Interface Sci.* **11** 273
Claesson P M, Poptoshev E, Blomberg E and Dedinaite A 2005 *Adv. Colloid Interface Sci.* **114** 173
[18] Doi M and Edwards S F 1986 *The Theory of Polymer Dynamics* (Oxford: Oxford University Press)
[19] de Gennes P G 1988 *Scaling Concepts in Polymer Physics* (Ithaca, NY: Cornell University Press)
[20] Wang Q 2005 *Macromolecules* **38** 8911
[21] Podgornik R and Saslow W M 2005 *J. Chem. Phys.* **122** 204902
[22] Fredrickson G 2006 *The Equilibrium Theory of Inhomogeneous Polymers* (Oxford: Oxford University Press)
[23] Manning G S 2006 *Biophys. J.* **91** 3607–16
[24] Strey H H, Wang J, Podgornik R, Rupprecht A, Yu L, Parsegian V A and Sirota E 2000 *Phys. Rev. Lett.* **84** 3105